J. Fluid Mech. (1993), *vol.* 249, *pp.* 287–305

Axisymmetric selective withdrawal in a rotating stratified fluid

By STEPHEN G. MONISMITH,[1] N. ROBB McDONALD[2]† AND JÖRG IMBERGER[2]

[1] Environmental Fluid Mechanics Laboratory, Stanford University, Stanford, CA 94305-4020, USA

[2] Department of Civil and Environmental Engineering and Centre for Water Research, University of Western Australia, Nedlands, 6009 WA, Australia

(Received 4 February 1992 and in revised form 16 October 1992)

In this paper we consider the axisymmetric flow of a rotating stratified fluid into a point sink. Linear analysis of the initial value problem of flow of a linearly stratified fluid into a point sink that is suddenly switched on shows that a spatially variable selective withdrawal layer is established through the outward propagation of inertial shear waves. The amplitude of these waves decays with distance from the sink; the e-folding scale of a given mode is equal to the Rossby radius of that mode. As a consequence, the flow reaches an asymptotic state, dependent on viscosity and species diffusion, in which the withdrawal-layer structure only exists for distances less than the Rossby radius based on the wave speed of the lowest mode, R_1. If the Prandtl number, Pr, is large, then the withdrawal layer slowly re-forms in a time that is $O(\delta_i^2 \kappa^{-1})$, such that it extends out much farther to a distance that is $O(R_1 Pr\, \delta_i^2 \delta_e^{-2})$ rather than $O(R_1)$.

Because there is no azimuthal pressure gradient to balance the Coriolis force associated with the radial, sinkward flow, a strong swirling flow develops. Using scaling arguments, we conclude that this swirl causes the withdrawal-layer thickness to grow like $(ft)^{\frac{1}{3}}$, such that eventually there is no withdrawal layer anywhere in the flow domain. Scaling arguments also suggest that this thickening takes place in finite-size basins.

These analyses of swirl-induced thickening and diffusive thinning can be combined to yield a classification scheme that shows how different types of flows are possible depending on the relative sizes of a parameter J, which we define as $fQ(Nh\nu)^{-1}$, E (the Ekman number $fh^2\nu^{-1}$), and Pr.

1. Introduction

It is well known that sink flows in rotating or stratified fluids tend to be jet-like in that the main part of the sinkward flow tends to come from narrow layers, either at the same level as the sink as in a strongly stratified fluid (Yih 1980) or along the rotational axis in a strongly rotating flow (Pao & Shih 1973). The former case is generically known as selective withdrawal in that in a strongly stratified fluid one can 'select' the strata of fluid at the sink level; this behaviour is often used to help manage reservoir water quality (Imberger 1980).

† Present address: Robert Hooke Institute, Clarendon Laboratory, Parks Road, Oxford, OX1 3PU, UK.

A novel application of selective withdrawal is described by Boyce, Robertson & Ivey (1983) who considered the possibility of selectively withdrawing 4 °C bottom water from Lake Ontario for use as cooling water to air-condition Toronto in summer. Their analysis, based on experimental and theoretical work by Whitehead (1980) and Kranenburg (1979, 1980) suggested that the so-called 'FREECOOL' scheme would not work because rotational effects would greatly increase the vertical extent of the withdrawal layer. The reasons for this were first laid out by Whitehead (1980) who analysed the flow of linearly stratified fluid into a point sink. Making approximate use of the rotating hydraulic control theory advanced by Whitehead & Porter (1977), Whitehead suggested that the withdrawal layer would first be established as in a non-rotating fluid† (assuming that N, the buoyancy frequency, is much greater than f, the Coriolis parameter). Later, owing to conservation of angular momentum, a swirling flow would develop that would require that fluid entering the sink have an ever increasing elevation head. Whitehead carried out several experiments to test his fully nonlinear, inviscid theory; generally the theoretical and experimental trends were in qualitative agreement. Most importantly, as predicted theoretically, the withdrawal-layer thickness increased significantly during all of his experiments.

In contrast to Whitehead's (1980) results, in their experimental study of selective withdrawal from a rotating channel, Monismith & Maxworthy (1989) failed to find any withdrawal-layer thickening. Like Whitehead, they used a point sink; however, their sink was mounted on one of the channel walls. They did observe, and analyse using a simple description of the evolution of the vertical vorticity field, the spinup of a strong recirculating flow. This flow developed because the emptying of the withdrawal layer acted to compress filaments of planetary vorticity, thus generating anticyclonic relative vorticity. This vorticity was diffused vertically by viscosity, leading to a apparent thickening of the withdrawal layer.

McDonald & Imberger (1992) analysed a flow related to that of Monismith & Maxworthy (1989): the flow into a line sink in a finite-depth, finite-width, and infinitely long duct. They confirmed the importance of Kelvin-wave/Poincaré-wave dynamics suggested by Monismith & Maxworthy (1989) based on Gill's (1976) analysis of the Rossby adjustment problem in a channel. In agreement with Monismith & Maxworthy (1989), they did not find any withdrawal-layer thickening despite the fact that non-zero velocities parallel to the sink developed as the flow evolved. This result differs from that found for flow into a line sink in an unbounded fluid, for which McDonald & Imberger (1991) calculated a spatially growing withdrawal layer.

In this paper, to clarify the nature of rotational effects on selective withdrawal, in particular to answer the question of when are spatial and temporal thickening of the withdrawal layer likely to be observed, we reconsider the problem analysed by Whitehead (1980): flow into a point sink. To simplify the analysis, we consider the deceptively simple case of a finite-depth, infinite-horizontal-extent fluid domain. We start, in §2, by looking at the inviscid, linear initial value problem associated with impulsively initiating the sink flow. The resulting solution, obtained by modal expansions and Laplace transforms, shows much what one would expect: the establishment of a withdrawal layer by long inertial-internal waves, which can be dubbed 'inertial shear waves' by analogy with their non-rotating counterparts (Pao & Kao 1974). However, the asymptotic form taken by the transient solution is not

† However, the no-rotation limit of Whitehead's analysis was not correct; see §3.

entirely expected in that it shows that the withdrawal layer vanishes at a distance of order Nh/f from the sink, where h is half the depth of the fluid. In §3, we next address the issue of temporal changes in withdrawal-layer thickness due to swirl using scaling arguments. In §4 we discuss the role played by viscous and diffusive effects. We note that all of our analyses are predicted on the assumptions that $N > f$, i.e. that the withdrawal layer is likely to extend horizontally rather than vertically (McDonald & Imberger 1991), and that transport to the sink from the interior takes place in the body of the fluid rather than in a thin Ekman layer on the basin bottom (as in Hide 1968). In §5 we develop a classification scheme delineating when viscous and diffusive effects are important. In §6 we apply our results to real reservoir flows.

2. The linear initial value problem: shear waves and selective withdrawal

We consider the flow induced in a linearly stratified fluid rotating at angular speed $\frac{1}{2}f$ about the z-axis by an impulsively started point sink. The sink is located at $(z, r) = (0, 0)$ and between horizontal free-slip planes at $z = \pm h$. The problem geometry is sketched in figure 1. In order to linearize the governing equations, we assume that the Froude number of the flow is small everywhere except in the immediate vicinity of the sink (Lawrence 1980; Imberger, Thompson & Fandry 1976; Ivey & Blake 1985). Likewise, if we assume that the horizontal scales of motion of interest are greater than the fluid depth (Pao & Kao 1974), we can neglect (for the moment – we will consider this point later) non-hydrostatic pressures. Finally, we neglect viscous and diffusive effects for the present time as well; they will be directly accounted for in §4.

In terms of the stream function, defined by the relations

$$u = \frac{1}{r}\psi_z, \quad w = -\frac{1}{r}\psi_r, \tag{1}$$

the equation governing the axisymmetric, small-amplitude motions associated with the establishment of a selective withdrawal layer is

$$\psi_{zztt} + f^2\psi_{zz} + N^2\left(\psi_{rr} - \frac{1}{r}\psi_r\right) = 0, \tag{2}$$

where N is the buoyancy frequency $(= -\rho^{-1}\rho_z)^{\frac{1}{2}}$. The stream function ψ is subject to the condition at $r = 0$ that

$$\lim_{r\to 0} \psi_z(r, z, t) = -\frac{Q}{2\pi} H(t)\,\delta(z), \tag{3}$$

where $H(t)$ is the Heaviside step function. Thus,

$$\lim_{r\to 0} \int_{-h}^{z} \psi_z(r, z, t)\, 2\pi\, \mathrm{d}z = 2\pi[\psi(0, z, t) - \psi(0, -h, t)] = -QH(t)\,H(z),$$

so that

$$\psi(0, z, t) = -\frac{Q}{2\pi} H(t)\,H(z) + \psi(0, -h, t). \tag{4}$$

If we set $\psi(0, -h, t) = QH(t)/4\pi$, this can be written as

$$\psi(0, z, t) = -\frac{Q}{4\pi} H(t)\,\mathrm{sgn}\,(z). \tag{5}$$

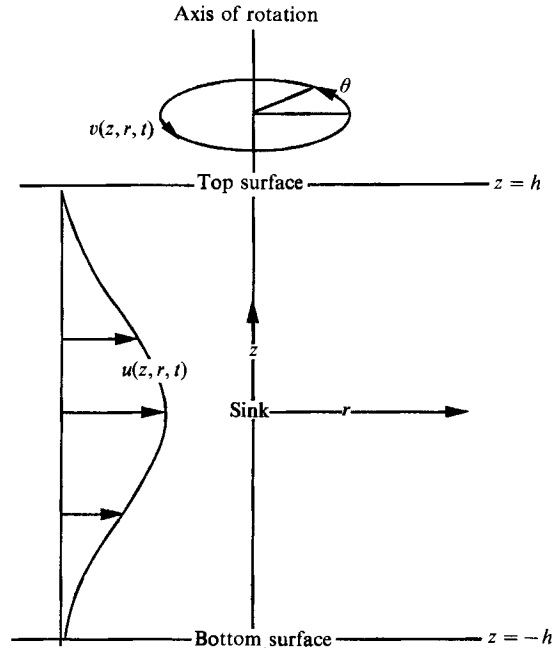

FIGURE 1. Definition sketch.

If the potential flow contribution to ψ is subtracted out, the remaining baroclinic portion of the stream function can then be expanded using ordinary modal expansions (Gill 1980):

$$\psi = -\frac{QH(t)}{4\pi}\frac{z}{h} + \sum_{n=1}^{\infty} f_n(r,t)\sin\left(\frac{n\pi z}{h}\right). \tag{6}$$

The sine expansion is used because sines are the appropriate eigenfunctions for a constant-N stratification (Gill 1980). Because $u \sim \psi_z$, $u \sim f_n$; i.e. u has the same (r,t)-dependence as do the f_n.

Making the following definitions:

$$z = hz^*; \quad r = \frac{Nh}{f}r^*; \quad t = f^{-1}t^*; \quad f_n = \frac{Q}{2\pi}f_n^*, \tag{7}$$

substituting the modal expansions into the field equation, and dropping the stars from dimensionless variables gives the radial wave equation for each of the modal amplitudes:

$$f_{n_{rr}} - \frac{1}{r}f_{n_r} - n^2\pi^2(f_{n_{tt}} + f_n) = 0. \tag{8}$$

The initial and boundary conditions on f_n can be obtained using the orthogonality of the modes to find that

$$f_n(0,t) = -\frac{1}{n\pi}H(t). \tag{9}$$

Equation (8) is solved by means of Laplace transforms. Taking the Laplace

transform of (8) gives the ordinary differential equation for the transformed variable $\bar{f}_n(s,r)$ (s is the argument of the transform):

$$\bar{f}_{n_{rr}} - \frac{1}{r}\bar{f}_{n_r} - n^2\pi^2(s^2+1)\bar{f}_n = 0, \tag{10}$$

which has the solution (given in Abramowitz & Stegun 1965)

$$\bar{f}_n = ArK_1[(s^2+1)^{\frac{1}{2}}n\pi r]. \tag{11}$$

K_1 is the modified Bessel function of the first kind. A is found by applying the initial condition, and noting that

$$\lim_{r\to 0}(ArK_1[(s^2+1)^{\frac{1}{2}}n\pi r]) = \frac{A}{n\pi(s^2+1)^{\frac{1}{2}}} \tag{12}$$

so that

$$A = -(s^2+1)^{\frac{1}{2}}/s. \tag{13}$$

Thus, the solution for $\bar{f}_n(s,r)$ is

$$\bar{f}_n = \frac{-(s^2+1)^{\frac{1}{2}}}{s} rK_1[(s^2+1)^{\frac{1}{2}}n\pi r]. \tag{14}$$

Inverting the Laplace transform gives

$$f_n(r,t) = -r\mathscr{L}^{-1}\left(sg(s)+\frac{1}{s}g(s)\right), \tag{15}$$

where the operator $\mathscr{L}^{-1}$ is used to signify the inverse Laplace transform and $g(s)$ is the function

$$g(s) = \frac{K_1[(s^2+1)^{\frac{1}{2}}n\pi r]}{(s^2+1)^{\frac{1}{2}}}. \tag{16}$$

Using the convolution theorem for Laplace transforms and the fact that $\mathscr{L}(f'(t)) = s\mathscr{L}(f)$, the solution for $f_n(r,t)$ can thus be written as (since $G(0)=0$)

$$f_n(r,t) = -r\left(\frac{\mathrm{d}G}{\mathrm{d}t} + \int_0^t G(\tau)\,\mathrm{d}\tau\right), \tag{17}$$

where $\mathscr{L}^{-1}(g(s)) = G(t)$. The formal solution can be completed by looking for the inverse transform of $g(s)$ in standard tables and finding that

$$\left.\begin{aligned} G(t) &= 0, && 0 \leqslant t < n\pi r, \\ G(t) &= \frac{\sin(t^2-(n\pi r)^2)^{\frac{1}{2}}}{n\pi r}, && t \geqslant n\pi r. \end{aligned}\right\} \tag{18}$$

Substituting this expression for G into the expression for f_n gives the full solution for the (r,t)-dependence of the modal amplitudes as

$$\left.\begin{aligned} f_n(r,t) &= 0, && 0 \leqslant t < n\pi r, \\ f_n(r,t) &= \frac{-t\cos(t^2-(n\pi r)^2)^{\frac{1}{2}}}{n\pi[t^2-(n\pi r)^2]^{\frac{1}{2}}} \frac{1}{n\pi}\int_{n\pi r}^{t} \sin(\tau^2-(n\pi r)^2)^{\frac{1}{2}}\,\mathrm{d}\tau, && t \geqslant n\pi r. \end{aligned}\right\} \tag{19}$$

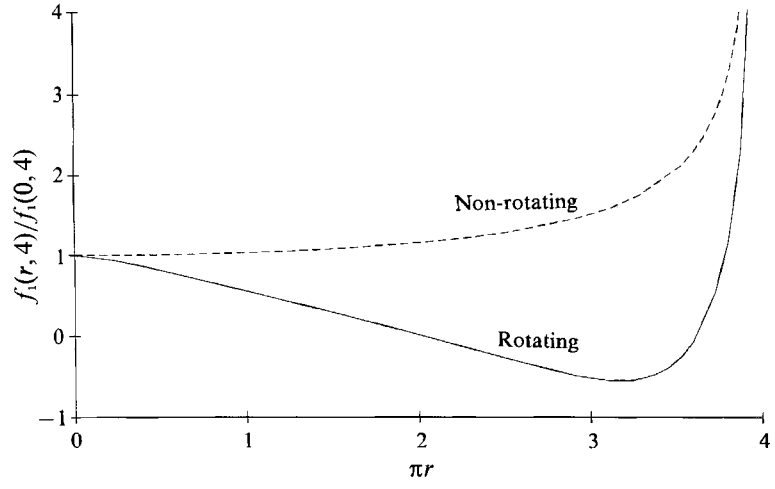

FIGURE 2. Radial structure of stream function at $ft = 4$ for rotating and non-rotating withdrawal layers for $n = 1$. Both have been made dimensionless by their values at the origin (which are the same) and the radial distance is scaled by π^{-1}.

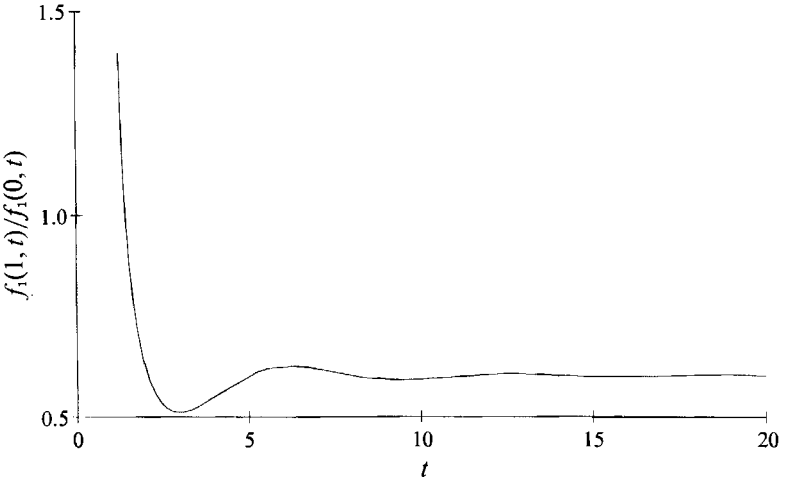

FIGURE 3. Time variation of $f_1(r,t)$ at $r = 1$ for $n = 1$ in the presence of rotation.

This solution, normalized by $f_n(0)$ is plotted on figure 2 for $t = 4$ and $n = 1$. For comparison, the non-rotating solution given by Lawrence (1980),

$$f_n(r,t) = 0, \qquad 0 \leqslant t < n\pi r,$$

$$f_n(r,t) = \frac{-t}{n\pi[t^2-(n\pi r)^2]^{\frac{1}{2}}}, \qquad t \geqslant n\pi r,$$

is also plotted. In both cases, at a given point in the fluid there is no response of the velocity field to the sink until a shear wave with dimensionless speed $(n\pi)^{-1}$ travelling outwards from the sink has reached that point. As plotted in figure 3 for $r = \pi^{-1}$ and $n = 1$, asymptotically, the rotating solution shows decaying inertial oscillations at fixed r. In both the rotating and non-rotating cases, the flow is singular at the wave front, essentially an artifact of the point-sink condition at $r = 0$, and of the neglect

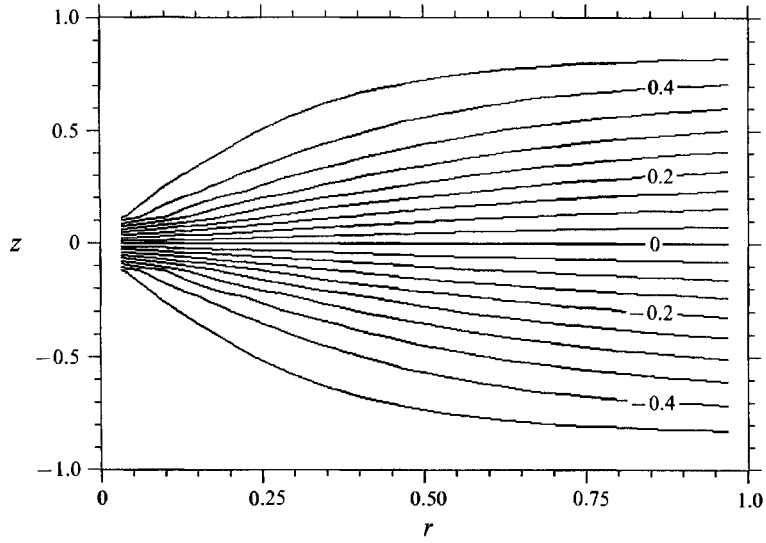

FIGURE 4. The asymptotic ($t \to \infty$) form of the inviscid flow field in terms of the dimensionless stream function.

of non-hydrostatic pressures. While a finite-radius sink could be included in the analysis to eliminate the singularity, it would greatly complicate the inversion of the Laplace transform while adding little information about flow behaviour away from the wave front.

The most interesting part of the solution is found by examining the asymptotic value of $f_n(r,t)$ as $t \to \infty$. This is easily done by letting $s \to 0$ in (16) and then inverting the approximation to $\bar{f}_n$ directly to find

$$f_n(r,t) \approx -rK_1(n\pi r). \tag{20}$$

This solution for ψ is plotted in figure 4 (including 10 modes) for $r < 1$. The most salient feature of this flow field is that the withdrawal structure existing near $r = 0$ virtually disappears by $r = 1$, i.e. a distance from the sink of approximately 3 times the Rossby radius of the lowest mode (π^{-1} in terms of the present set of dimensionless variables). In contrast, in the non-rotating case, the withdrawal-layer structure established at the sink is maintained throughout the fluid.

Strictly speaking, this limiting process for finding the large-time behaviour of the Laplace transform is valid only when the singularities of the Laplace transform do not lie on the imaginary axis. Such is not the case here. However, this problem can be eliminated with the inclusion of a small amount of linear drag, ϵ; i.e. by replacing $\partial/\partial t$ by $\partial/\partial t + \epsilon$. Such a transformation lifts the singularities off the imaginary axis, making the above limiting process valid. The limit $\epsilon \to 0$ can then be taken to obtain the inviscid solution (McDonald 1992). By substituting (20) into the modal expansion, we arrive at an asymptotic expression for the dimensionless steady-state flow.

The reason for this loss of selective withdrawal is clear from the asymptotic behaviour of K_1. Since

$$rK_1(n\pi r) \approx (r/2n)^{\frac{1}{2}} e^{-n\pi r} \tag{21}$$

for $r \gg 1$, we see that nth mode's contribution to the velocity field decays exponentially with an e-folding scale equal to $(n\pi)^{-1}$, the dimensionless Rossby

radius for that mode. Thus, as first described by McDonald & Imberger (1991), we must conclude that the vertical scale of the withdrawal layer set up by outward-propagating inertial shear waves increases with distance from the sink. This is because the farther we are from the sink, the smaller the contribution to the velocity field made by the higher modes.

Finally, for completeness, we can write asymptotic expressions for the dimensional forms of ψ and u, valid for $t \gg f^{-1}$, by reconstruction of the modal expansions and by the use of (1) which connects u and ψ. These are

$$\psi \approx \frac{-Q}{2\pi}\left(\frac{z}{2h}+\frac{fr}{Nh}\sum_{n=1}^{\infty} K_1\left(\frac{n\pi fr}{Nh}\right)\sin\left(\frac{n\pi z}{h}\right)\right) \tag{22}$$

and

$$u \approx \frac{-Q}{2\pi h^2}\left(\frac{h}{2r}+\frac{f}{N}\sum_{n=1}^{\infty} n\pi K_1\left(\frac{n\pi fr}{Nh}\right)\cos\left(\frac{n\pi z}{h}\right)\right). \tag{23}$$

The slow convergence of the series expression (23) for u for $r \approx 0$ is entirely the result of the assumed delta-function sink structure. Much more rapid convergence of this series could be obtained by assuming a sink distribution appropriate to the withdrawal-layer velocity structure that is established near the sink (Monismith, Imberger & Billi 1988).

3. Evolution of the swirl: to select or not to select?

In the context of the linear, inviscid analysis given in §2, the swirl, v, can be easily computed from the θ-momentum equation

$$v_t = -fu. \tag{24}$$

Integrating (24) with respect to t and assuming that $v = 0$ at $t = 0$, we find that

$$v = -ftu_s, \tag{25}$$

where u_s is the steady velocity field given in (23). However, as v grows with time, the flow field is not steady. In fact, (25) implies that the radial pressure gradient near the sink must also increase with time since for $t \gg f^{-1}$,

$$-fv-\frac{v^2}{r} = -\frac{1}{\rho}p_r. \tag{26}$$

Thus, the perturbation pressure also grows with time. Since the perturbation pressure is derived from deflection of the isopycnals, we might suppose that this implies that the withdrawal layer must grow in thickness with time. Indeed, this is exactly the conclusion drawn by Whitehead (1980) from his analysis of the present flow.

We can examine this conclusion using scaling arguments. First consider the non-rotating case: we assume that the withdrawal-layer thickness near the sink, δ_i, is initially set by an inertia–buoyancy balance, wherein a radial pressure gradient

$$\rho^{-1}p_r \sim N^2\delta_i^2/R \tag{27}$$

(R is the appropriate radial lengthscale) is balanced against inertia

$$uu_r \sim Q^2\delta_i^{-2}R^{-3}. \tag{28}$$

Run	Q ($cm^3\ s^{-1}$)	N (s^{-1})	T (s)	f (s^{-1})	δ_i (cm)	$\frac{Nh}{fR_0}$	J	E $\times 10^5$	Pr
1	0.20	1.45	10	1.26	0.52	0.5	1.16	4.4	700
2	0.20	1.45	20	0.63	0.52	1.0	0.58	2.2	700
3	0.20	1.45	60	0.21	0.52	2.1	0.19	1.5	700
4	2.50	1.45	355	0.04	1.20	18	0.41	1.1	700

TABLE 1. Whitehead (1980)'s experimental data

Following Ivey & Blake's (1985) argument, we expect that the withdrawal layer is established within a distance of order δ of the sink so that $R \sim \delta$, implying that

$$\delta_i \sim (Q/N)^{\frac{1}{3}}. \tag{29}$$

As suggested by Whitehead, the magnitude of the swirl is of paramount importance for the rotating case. It would appear that our ability to use the linear estimate (25) to calculate v would be limited in that v appears to increase without bound and thus it should be necessary to account for advection of v. On the other hand, if (25) was a valid basis for scaling v, we would find that

$$v \sim Qft/\delta r. \tag{30}$$

As discussed in the Appendix, this scaling is, in fact, correct for a constant-thickness withdrawal layer, since for $u_s \sim r^{-1}$, the two horizontal advection terms in the θ-momentum cancel identically. This temporally increasing velocity implies that near the sink, where the withdrawal layer is established,

$$\frac{fv}{v^2/r} \sim \frac{fr}{v} \sim \frac{\delta r^2}{tQ} \sim \frac{\delta^3}{tQ} \sim (Nt)^{-1}, \tag{31a}$$

while a comparison of the relative sizes of the centripetal and advective accelerations shows that

$$\frac{u(\partial u/\partial r)}{v^2/r} \sim \frac{u^2}{v^2} \sim (ft)^{-2}. \tag{31b}$$

Thus, for $t \gg f^{-1}$, the flow near the sink must be in cyclostrophic balance, i.e.

$$\frac{v^2}{r} \approx \frac{1}{\rho} p_r. \tag{32}$$

Keeping the scaling of the pressure gradient specified by (27), assuming again that $R \sim \delta_r$ (the subscript r refers to rotation), but now assuming the appropriate radial momentum balance is (32) and noting that

$$v \sim ftQ/\delta_r^2, \tag{33}$$

we find that $$f^2t^2Q^2\delta_r^{-5} \sim N^2\delta_r,$$

so that $$\delta_r \sim (ft)^{\frac{1}{3}}(Q/N)^{\frac{1}{3}}. \tag{34}$$

Equation (30) implies that $$\delta_r/\delta_i \sim (ft)^{\frac{1}{3}}. \tag{35}$$

Thus, not only should we expect the withdrawal layer to grow with distance because of rotation, but also with time. The appearance $t^{\frac{1}{3}}$ growth in (35) rather than $t^{\frac{1}{2}}$ as predicted by Whitehead is because he assumed line-sink behaviour with $u \sim Q(\delta r_0)^{-1}$, where r_0 was the radius of the outlet, rather than point-sink dynamics with $u \sim Q\delta^{-2}$

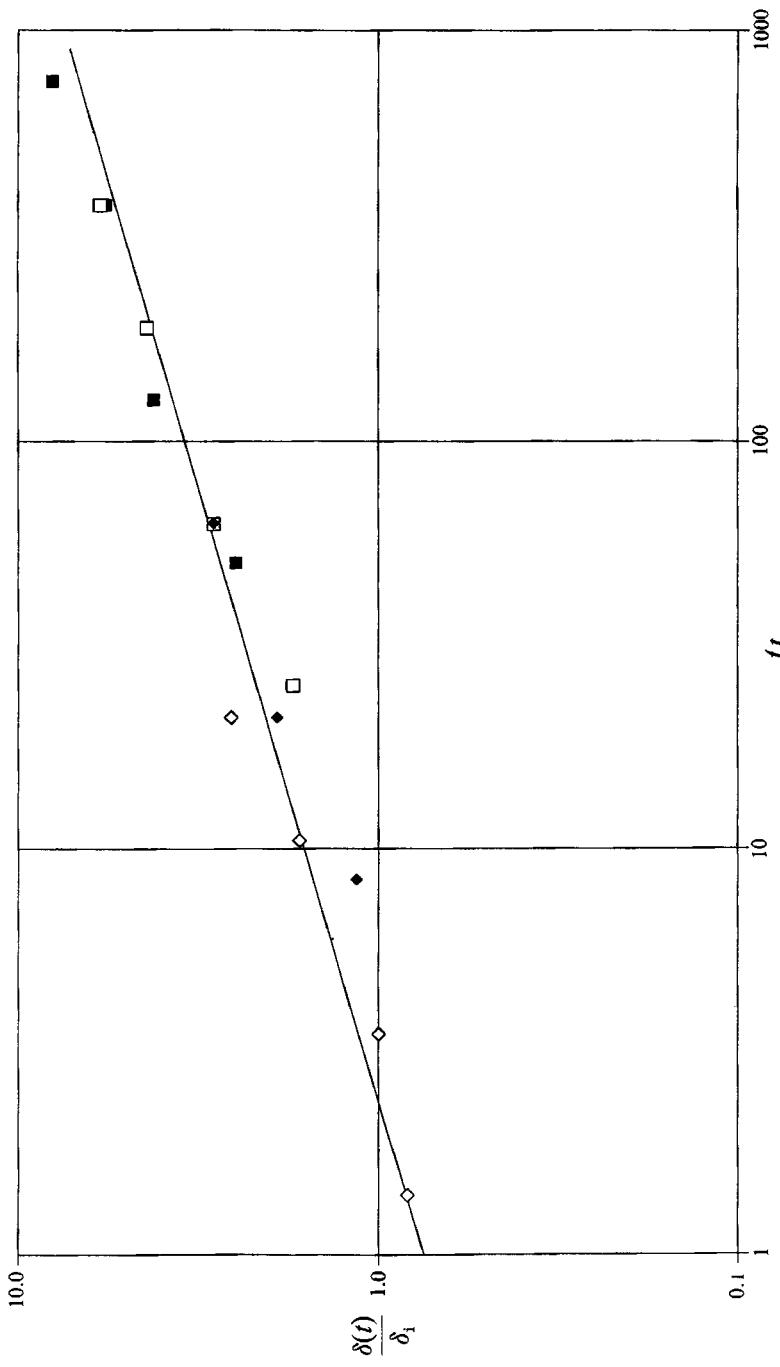

FIGURE 5. Inertia–rotation scaling of Whitehead's experimental data: Run 1 (■); Run 2 (□); Run 3 (◆); Run 4 (◇). The solid line is (35) with a constant of proportionality of 0.7.

(see Ivey & Blake 1985). We expect that Whitehead's analysis should be valid when $r_0 > \delta_r$.

As noted by Whitehead, the dominance of the cyclostrophic pressure balance over geostrophy (in the radial direction) is appealing in that it means that the withdrawal-layer behaviour is consistent with the Bernoulli equation interpretation that is traditionally given to inertial layers (see e.g. Yih 1980): The drawndown of isopycnals near the sink represents the conversion of elevation head into velocity head that is often found in open channel flow. Since the Coriolis force does not enter the Bernoulli equation directly (it acts at right angles to streamlines), this interpretation would not hold had radial geostrophy determined the withdrawal-layer thickness.

To what extent can the analysis given above be tested against experimental data? The only data set we are aware of is that of Whitehead, which is summarized in table 1 (we have only chosen those experiments that geometrically correspond to the problem at hand). Whitehead's results are plotted in figure 5, which it can be seen that the scaling given by (35) does an excellent job at collapsing the experimental data. Using these data, the coefficient of proportionality for (35) appears to be approximately 0.7. It should be pointed out that in the case of Whitehead's experiments, one would not have expected to see much spinup due to withdrawal-layer depletion because, in all cases, the time required to empty the withdrawal layer, and hence create vertical vorticity through the compression of planetary vortex filaments, was somewhat longer than the time the experiments were run.

Another facet of this description that can be checked is that (25) implies that v is positive since u_s is negative. While the data given by Whitehead cannot be used to confirm this prediction, the bead-streak image given in Monismith & Maxworthy (1989) do show a region of counterclockwise flow around the sink which is imbedded in the otherwise clockwise flow spun up by the withdrawal-layer flow. In their case, the sink was placed a small distance from the wall, allowing a small amount of swirl to develop. Apparently, this swirl was not sufficient, however, to lead to any observable thickening of the withdrawal layer.

An important aspect of (35) is that it predicts no selective withdrawal if $\delta_r \sim h$. That is, when $t = T_r$, the time by which selective withdrawal has ended because of rotation:

$$(ft)^{\frac{1}{3}}(Q/N)^{\frac{1}{3}} \sim h,$$

or

$$fT_r \sim Nh^3Q^{-1},$$

which is equivalent to the statement that

$$fT_r \sim Fr^{-1}, \tag{36}$$

where the Froude number Fr is defined as

$$Fr = QN^{-1}h^{-3}. \tag{37}$$

Suppose now that the fluid domain is a cylinder of radius R_0. According to our solution above (e.g. given by (22) and (23)), we would expect that the 'rear' wall will have little effect on the 'steady-state' flow so long as

$$R_0 \gg Nh/f.$$

The major effect of the rear wall will be to cause a drawndown of the water level as fluid is removed from the cylinder. This naturally defines an emptying time

$$T_E \sim hR_0^2Q^{-1}. \tag{38}$$

Thus if $T_r \ll T_E$, the fluid density structure will change as though stratification were not present, i.e. as if there were no selective withdrawal. Thus, for this to be the case we must specify that

$$N/f \ll (R_0/h)^2$$

or equivalently that

$$Nhf^{-1} \ll R_0 \tag{39}$$

as assumed above. Thus, our scaling arguments predict that a large finite-radius basin will not experience significant selective withdrawal during the time it is emptied.

4. Effects of viscosity and species diffusion

The linear inviscid analysis can be extended to include diffusion of momentum and of species while retaining the modal structure of the flow. However, we must retain the assumptions that the top and bottom boundaries are slip boundaries and allow weak fluxes to pass through them. In this case (10), which describes the radial structure of a Laplace-transformed modal stream function, becomes

$$\bar{f}_{n_{rr}} - \frac{1}{r}\bar{f}_{n_r} - n^2\pi^2 \frac{(s+Pr^{-1}E_n)\,((s+E_n)^2+1)}{s+E_n}\bar{f} = 0, \tag{40}$$

where Pr is the Prandtl number $= \nu/\kappa$ (ν is the kinematic viscosity and κ the thermal diffusivity) and E_n is the 'modal Ekman number' which is defined by the expression

$$E_n = (\nu/f)\,(n\pi/h)^2. \tag{41}$$

The modal Ekman number, which is just the product of the Ekman number, E

$$E = \nu/fh^2 = \delta_e^2/h^2, \tag{42}$$

and $(n\pi)^2$, is the square of the ratio of the Ekman-layer thickness, δ_e, to the vertical lengthscale of the nth mode.

The solution to (40) is similar to that given above:

$$\bar{f}_n = -(\lambda_n/s)\,rK_1(\lambda_n\, n\pi r). \tag{43a}$$

Here the effects of diffusion and rotation are expressed by the function

$$\lambda_n(s, E_n, Pr) = \left\{\frac{(s+Pr^{-1}E_n)\,((s+E_n)^2+1)}{s+E_n}\right\}^{\frac{1}{2}}. \tag{43b}$$

A general inversion of (43) is complicated, so it is preferable to look at the long-time behaviour of the solution. However, for reasons that will become apparent below, some care needs to be taken when evaluating limiting forms of (43) and its inverse.

The first case is to let $s \to 0$ while keeping Pr and E fixed. Velocity profiles for $E = 0.1$ and $Pr = 1$, 10 and 100 at $r = 1$ are shown in figure 6. While it is not shown, the inviscid velocity profile is indistinguishable from the $Pr = 1$ case. In contrast, the velocity profile for $Pr = 10$ is much more like that seen in the absence of rotation, i.e. it shows selectivity. This behaviour is seen in the asymptotic limit of f_n which, for $Pr \to \infty$ (and E fixed), is

$$f_n \sim -(n\pi)^{-1}; \tag{44}$$

i.e. the non-rotating solution of Lawrence (1980). More generally, keeping both E and Pr fixed and letting $s \to 0$ gives for the Laplace inversion

$$f_n(r, t \to \infty) \approx -\left(\frac{E_n^2+1}{Pr}\right)^{\frac{1}{2}} rK_1\left(\left(\frac{E_n^2+1}{Pr}\right)^{\frac{1}{2}} n\pi r\right), \tag{45}$$

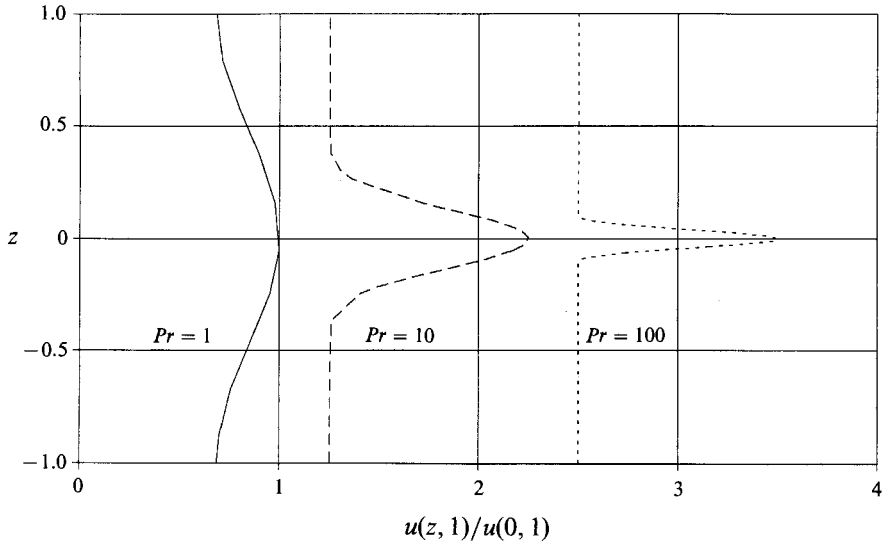

FIGURE 6. Dimensionless asymptotic ($t \to \infty$) velocity profiles at $r = 1$ for $E = 0.1$, and various values of Pr. Each profile has been normalized by $u(z = 0, r = 1)$ and the profiles for $Pr = 10$ and 100 have been shifted to the right by 1.25 and 2.5 respectively.

which is identical to (20) except for the rescaling of the radial distance by the factor

$$\beta_n = \left(\frac{E_n^2 + 1}{Pr}\right)^{\frac{1}{2}} \tag{46}$$

which for $E_n \ll 1$, is just $Pr^{-\frac{1}{2}}$. Thus, the steady form of the rotationally decaying withdrawal layer would appear to extend out much farther than predicted in §2.

However, an alternative limiting solution obtained by first letting $E \to 0$ while keeping Pr fixed, and then taking $s \to 0$ gives the inviscid solution described in §2. The question is: which limit is correct? The answer would appear to lie in what timescale is of interest. Ultimately, the diffusive solution must be realized if Froude number is sufficiently small (Imberger *et al.* 1976). This is because the 'steady' inviscid solution does not give a steady density field since $w \neq 0$. The inviscid limit appears to be appropriate for

$$1 \ll t \ll E_n^{-1}, \tag{47}$$

because in this case, we can neglect all the diffusive contributions to (43), while still considering t to be large enough for the small-s limit of the solution to be valid. For longer times, such that

$$E_n^{-1} \ll t \ll Pr\, E_n^{-1}, \tag{48}$$

viscous effects must be included, while diffusion of species can still be neglected. This gives the velocity field described by (44). Finally, for

$$Pr\, E_n^{-1} \ll t \tag{49}$$

the full diffusive solution given by (45) will hold. Thus, in summary, it would appear that, like the non-rotating case, if $Pr > 1$ the inviscid flow described in §2, which is first established by shear waves, will evolve further until it reaches a diffusive equilibrium with a withdrawal layer that is thinner at fixed r than if there were no diffusion.

Physically, the balance of forces and effects involved with this collapse appears to be as follows: After the inviscid/non-diffusive flow is established, the density

Time	λ_n	Force balance	Layer scale
$1 \ll t \ll E_n^{-1}$	1	$fv \sim p_r/\rho_0$ $v_t \sim fu$ $\rho_t \sim \rho_0 N^2 w/g$	$\delta \sim fRN^{-1}$
$E_n^{-1} \ll t \ll Pr E_n^{-1}$	$(s/N)^{\frac{1}{2}}$	$fv \sim p_r/\rho_0$ $fu \sim \nu v_{zz}$ $\rho_t \sim \rho_0 N^2 w/g$	collapses
$Pr E_n^{-1} \ll t$	$Pr^{-\frac{1}{3}}$	$fv \sim p_r/\rho_0$	$\delta \sim fR Pr^{-\frac{1}{2}} N^{-1}$

TABLE 2. Force balances and withdrawal-layer thicknesses (linear theory)

perturbation increases as the swirl increases. As the swirl develops, it is also diffused by viscosity. This causes the required density perturbation to decrease; since the density perturbation is proportional to the isopycnal displacement, i.e. the withdrawal-layer thickness, the withdrawal layer must thin. Ultimately, in the absence of advection of either species or momentum, the withdrawal layer becomes sufficiently narrow for species diffusion to end the growth of the density perturbation and thus finally allow the withdrawal flow to become steady. For very large values of Pr, this will result in a layer that is at most as thick in the body of the fluid as it is at the sink itself where the dominant force balance may still be between inertia and buoyancy. This discussion is summarized in table 2 where we present a compilation of the various timescales and their associated force balances and withdrawal-layer thicknesses.

It should be noted that (49) and the equations that precede it involve E_n rather than E. This means that with E fixed, at time t, all modes with $E_n^{-1} < t$ will show viscous influence. Fortunately, this is not a severe constraint: if the withdrawal layer has finite thickness δ at the sink due to inertial effects, then the largest value of E_n that need be considered, the one that will set the time for which the inviscid solution given in §2 is useful, will be the one for which

$$E_n \approx \nu(f\delta_i^2)^{-1} = (\delta_e/\delta_i)^2. \tag{50}$$

That is, n is chosen such that the Ekman number of the nth mode is comparable to the square of the ratio of the Ekman-layer thickness to the withdrawal-layer thickness. This is because the finite thickness of the withdrawal layer near the sink reduces the amplitudes of the higher modes relative to those values appropriate to a delta-function sink (Imberger *et al.* 1976). We discuss below the implications of viscous and diffusive effects for the long-time behaviour of the flow.

5. Discussion and classification of flows

The analyses presented in the previous three sections have delineated a series of different dynamical balances including advection, rotation and diffusive effects. To proceed further we need to decide on what types of flow evolution are possible. Thus, we wish to consider how the different flow descriptions might be combined to yield a comprehensive view of sink flow in a rotating stratified fluid. In particular, how do we reconcile the picture of a rotationally thickening layer given in §3 with the viscously/diffusively collapsing layer described in §4? The key to answering this question is to realize that even when viscosity and diffusion are important in the interior of the domain (away from the sink), they cannot make the withdrawal layer

thinner in the interior than it is at the sink. Since the speed of the inertial shear waves is proportional to the vertical wavelength and it is this vertical wavelength that locally determines the withdrawal-layer thickness it follows that when steady state is achieved, say through diffusion of such waves by viscosity, the withdrawal-layer thickness cannot decrease with distance from the sink.

First, to ensure a layer that is initially inertial, the withdrawal layer must be established before viscous effects become important. Given that the appropriate timescale for establishment of an inertial layer is $O(N^{-1})$ near the sink and that the viscous timescale is $O(\delta_1^2 \nu^{-1})$, we require that

$$N\delta_1^2 \nu^{-1} > 1. \tag{51}$$

If we define the parameter

$$J = Qf(Nh\nu)^{-1}, \tag{52}$$

we find that the necessary condition is

$$J > f^{\frac{3}{2}} N^{-\frac{3}{2}} E^{\frac{1}{2}}. \tag{53}$$

Next, in order to see the inviscid flow analysed in §2, we must retain an inertial layer near the sink while the flow away from the sink is established. This means that the viscous timescale must be greater than the time required for the appropriate internal wave mode to travel the characteristic dimension of the basin (Ivey & Blake 1985). In this case, the setup time is identical for all modes since the appropriate lengthscale for each mode is its Rossby radius, so the necessary condition is now

$$f\delta_1^2 \nu^{-1} > 1, \tag{54}$$

which, expressed in terms of J, is

$$J > E^{\frac{1}{3}}. \tag{55}$$

Once the initial spatially growing withdrawal layer has been established, our analysis (§§2–4) suggest two possibilities: the layer grows with time near the sink due to rotation, and hence in the interior as well; the layer in the interior collapses vertically such that at any particular distance from the sink, the local layer thickness becomes smaller with time until it reaches a limiting scale set by diffusion of species and momentum and by the withdrawal-layer thickness near the sink. If we combine these two possible descriptions, we must infer that if the viscous/diffusive effects remain unimportant near the sink, the withdrawal layer grows as described in §3 with the interior flow matching it either with the geostrophic balance described in §2, or with the viscous/diffusive balance discussed in §4. By looking at the various force balances and timescales, we can determine what type of flow should arise, depending on J, E, and Pr.

First, to guarantee a rotational layer near the sink, $\nu v_{zz} < v^2 r^{-1}$. This gives

$$(ft)^{\frac{2}{3}} N\delta_1^2 \nu^{-1} > 1. \tag{56}$$

Since $ft > 1$ for the cyclostrophic balance to hold in the first place, we find that if the layer is initially inertial, it will also be cyclostrophic for all $ft > 1$.

The cyclostrophic balance will continue until the layer has grown to fill the entire depth, i.e. for $t < T_r$. Thus, the importance of viscosity and species diffusion to the evolving flow will depend on the extent to which the layer can fill the basin depth before viscous and or diffusive effects act. In the limit where the vertical lengthscale of the flow is h, we find that viscous/diffusive effects will never be important if

$$fT_r < fh^2\nu^{-1} = E^{-1}. \tag{57}$$

This criterion gives the condition $J > 1$ (58)

as defining the boundary between flows for which viscosity may or may not be important. If $J < 1$, it is easily shown that the transition time at which viscous effects become important is $O(f^{-1}J^2E^{-1})$. Diffusive effects in the interior will come into play during the spinup and thickening of the withdrawal layer if

$$fT_r < fh^2\kappa^{-1} = E^{-1}Pr, \tag{59}$$

or if

$$J < Pr^{-1}. \tag{60}$$

Thus, in order that the interior flow be able to make the transition from geostrophy to a viscous–diffusive equilibrium, there is the auxiliary condition that $Pr^{-1} > E^{\frac{1}{2}}$. This flow is slightly different from that discussed in §4 in that the layer thickness is set by the dynamics of the flow near the sink.

Summarizing the above results, we can describe several different regimes of flow behaviour when $Pr^{-1} > E^{\frac{1}{2}}$:

(i) $J > 1$: the flow is initially inertial and remains inviscid until selectivity is lost due to rotation;

(ii) $1 > J > Pr^{-1}$: the flow is inertial/rotational near the sink, but the spinup of the interior flow is modified by viscosity;

(iii) $Pr^{-1} > J > E^{\frac{1}{2}}$: the flow is inertial/rotational near the sink, but the spinup of the interior flow is modified by viscosity and species diffusion;

(iv) $E^{\frac{1}{2}} > J > f^{\frac{3}{2}}N^{-\frac{3}{2}}E^{\frac{1}{2}}$: the flow is inertial/rotational near the sink but viscosity modifies the establishment of the flow;

(v) $f^{\frac{3}{2}}N^{-\frac{3}{2}}E^{\frac{1}{2}} > J$: the flow is never inertial (this case is discussed in §4). If $Pr^{-1} < E^{\frac{1}{2}}$, regime (iii) flows cannot be realized, but the rest of the classification scheme holds.

If we again look at Whitehead's (1980) experiments (see table 1), we find that his experiments fall on the boundary separating regimes (i) and (ii). Thus, our classification scheme would lead us to conclude that the withdrawal layers he produced should have been inertial initially, and, as he observed, should have subsequently thickened owing to rotation. Moreover, as Whitehead suggested through scaling, viscosity probably had little effect on the flow.

6. Discussion

To put our results in perspective, we consider the application of our results to flows in large lakes and reservoirs. We limit our attention to the inviscid, non-diffusive case only. A large lake might have the following characteristic parameter values (for mid-latitudes): $N \sim 10^{-2}\ \mathrm{s}^{-1}$ (roughly 1 °C m^{-1}); $f = 10^{-4}\ \mathrm{s}^{-1}$; $Q \sim 1\ \mathrm{m}^3\ \mathrm{s}^{-1}$; $H \sim 100$ m; and $R_0 \sim 10$ km. If we estimate a value of $10^{-4}\ \mathrm{m}^2\ \mathrm{s}^{-1}$ for an effective value of viscosity in the hypolimnion of a lake (Ivey & Imberger 1976), $J \sim 1$ and $NH/f \sim 10\ \mathrm{km} \sim R_0$ so that we would conclude that the withdrawal flow should develop first as described by the linear inviscid model and then eventually lose much of its structure altogether due to swirl-induced withdrawal-layer thickening.

For a smaller lake or reservoir, R_0 might be smaller than the lowest-mode Rossby radius Nh/f, in which case our analyses do not strictly apply. However, it seems likely that some of the spatial thickening discussed in §2 might be observed if R_0 is comparable to, although less than, Nh/f. Moreover, since δ_r is at most $O(H)$, temporal thickening of the withdrawal layer might still be expected to occur much as discussed in §3 given that the flow dynamics that determines δ_r is, in large part, local to the sink. This seems confirmed by the fact that Whitehead's experiments were performed

in a tank in which the Rossby radius of the lowest mode was varied from being roughly equal to the tank radius (experiment 1) to being much greater than the tank radius (experiment 4), yet there is no discernable difference in their dimensionless layer growth rates.

This potential importance of rotation to selective withdrawal for moderate size lakes and reservoirs also suggests an important design rule for selective withdrawal intakes: in a large lake, in order to maintain any 'selectivity', the withdrawal structure must be placed within one or two Rossby radii of the lowest internal wave mode of the shore. In general, in order to have the ability to produce as narrow a layer as possible and so gain the maximum degree of control of the outflow, the structure should be positioned so as to prevent the development of swirl around the structure. Practically speaking, for water supply reservoirs this would generally mean positioning the structure close to the dam wall if bottom water is to be selectively withdrawn, given that the water depth is usually greatest near the dam.

Another flow of practical interest is that of a sink flow induced by a bubble plume in a small reservoir with $H = 10$ m and $R_0 = 500$ m. The strength of this sink varies with height, effectively appearing like a distributed form of the point sink analysed above (McDonald 1992). Will the variation in sink strength be felt over the entirety of the reservoir? In this case, $NH/f = 1000$ m, so that much of the detailed structure of the plume's entrainment flow might disappear due to rotation. The importance of rotation at these scales is not unexpected. Indeed Kranenburg's (1979) analysis of rotating sink flow was originally motivated by the observation that significant swirl developed around bubble plumes in basins of approximately this scale.

Lastly, the question of stability of the withdrawal flows discussed in this paper is open, although given that neither Kranenburg (1979, 1980) nor Whitehead (1980) commented on the development of instabilities in the asymmetric cases they studied, it seems likely that none occurred and thus that some withdrawal flows might be stable. More discussion of rotational instabilities can be found in Gill (1980).

7. Conclusions

The analysis given herein suggests both by formal solution and by scaling arguments, that rotational effects on axisymmetric selective withdrawal might be substantial, including a spatially variable withdrawal layer that decays with distance from the sink such that for distances of order Nh/f, there is no withdrawal layer. Examination of the inviscid swirling flow that evolves for large times ($t \gg f^{-1}$) suggests that under many conditions of interest, all 'selectivity' of the withdrawal layer may be lost. In this case, the withdrawal-layer thickness grows like $(ft)^{\frac{1}{3}}$. For example, finite-size basis that are several times wider than the Rossby radius of the lowest-mode interval wave will most likely experience little, if any, selective withdrawal as they empty. According to linear analysis, this picture may be modified by the presence of diffusion of species and of momentum; for $Pr \gg 1$, the withdrawal layer collapses with time such that a narrow withdrawal layer is re-established by $t = O(\delta_1^2 \kappa^{-1})$. However, in general, the evolution of the flow depends on the parameter J defined in §5, and a variety of flows are possible depending on the relative sizes of J, E, the Ekman number and Pr, the Prandtl number.

S.G.M. is supported by NSF through grant CTS 8958314 and by a gift from the Charles Lee Powell Foundation. N.R.M. was supported by the Centre for Environmental Fluid Dynamics at the University of Western Australia.

Appendix. An exact solution for the θ-momentum equation

In §3, an estimate for the swirl (θ) velocity, v was given by the expression (30):

$$v \sim Q(ft)/\delta(t)\, r,$$

where $\delta(t)$ is the withdrawal-layer thickness. In this section, we justify this scaling by obtaining an exact solution of the θ-momentum equation that has the form given by (30).

We consider the unsteady, vertically uniform flow inside a withdrawal layer of constant thickness $\delta(t)$. The sinkward flow is assumed to only vary slowly in time (as a result of withdrawal-layer thickening – represented here by allowing δ to be a function of time) according to the relation:

$$u = -Q/2\pi\,\delta(t)\, r. \tag{A 1}$$

In this flow, the vertical velocity is identically zero and thus, neglecting viscosity, the θ-momentum equation simplifies to the form

$$\frac{\partial v}{\partial t} = -u\left(f + \frac{v}{r} + \frac{\partial v}{\partial r}\right). \tag{A 2}$$

The steady form of this equation was used by Whitehead (1980) in his analysis.

The neglect of wv_z can be justified by noting that the vertical velocity w, should be $O(QA^{-1})$, where A is the area of the basin, in order that the density field only change slowly in response to the evolving swirl. This estimate for w gives $wv_z = O(QvA^{-1}\delta^{-1})$ as opposed to uv_r being $O(Qv\delta^{-3})$. This simplifies that $wv_z \ll uv_r$ and can thus be neglected since $wv_z/uv_r = O(\delta^2 A^{-1})$ and $\delta \ll A^{\frac{1}{2}}$. Spigel & Farrant (1984)'s experiments and analysis indicate that this scaling gives a good description of the flow field for non-rotating inertial withdrawal flow. In addition, Monismith & Maxworthy (1989) successfully used the same vertical velocity field as Spigel & Farrant to model spinup in a rotating selective withdrawal flow. Finally, this assumption would seem to be consistent with Whitehead's description of the withdrawal layer (p. 129) that 'There was little change in depth [of the layer] away from the sink'.

An exact solution to (A 2) is easily obtained by noting that if $v \sim r^{-1}$, then the last two terms on the right-hand side of (A 2) cancel identically leaving the simple spinup balance:

$$\partial v/\partial t = -fu. \tag{A 3}$$

If withdrawal-layer thickness is

$$\delta(t) = \delta_0 (ft)^n \tag{A 4}$$

then the solution to (A 3) is

$$v = Q(ft)/((1-n)\, 2\pi\, \delta(t)\, r). \tag{A 5}$$

As discussed in the §3, a balance of the radial pressure gradient and the centripetal acceleration gives $n = \frac{1}{3}$.

This solution has a simple interpretation in terms of conservation of angular momentum. As Whitehead (1980) argued, at time t, we see at r a ring of fluid that was initially at a distance r_0 where

$$\tfrac{1}{2} r_0^2 = \tfrac{1}{2} r^2 + Qt/(2\pi\,\delta(1-n)). \tag{A 6}$$

Equation (A 6) is obtained by integration of (A 1). Thus, using (A 5) we can write that

$$rv = \tfrac{1}{2} f r_0^2 - \tfrac{1}{2} f r^2. \tag{A 7}$$

However, the angular momentum, H_z, of the fluid ring as measured in an inertial reference frame, is

$$H_z = rv + \tfrac{1}{2}fr^2 = \tfrac{1}{2}fr_0^2, \tag{A 8}$$

which is constant. Thus, the swirl described by (30) or (A 5) develops because, as fluid rings move towards the sink, they must develop additional positive θ-velocity in order to conserve angular momentum.

REFERENCES

ABRAMOWITZ, M. & STEGUN, I. A. 1965 *Handbook of Mathematical Functions*. Dover.

BOYCE, F. M., ROBERTSON, D. G. & IVEY, G. N. 1983 Summer thermal structure off Lake Ontario: Cooling the big city. *Atmos. Ocean* **21**, 397–417.

GILL, A. E. 1976 Adjustment under gravity in a rotating channel. *J. Fluid Mech.* **77**, 603–621.

GILL, A. E. 1980 *Atmosphere-Ocean Dynamics*. Academic.

GREENSPAN, H. P. 1968 *The Theory of Rotating Fluids*. Cambridge University Press.

HIDE, R. 1968 On source-sink flows. *J. Fluid Mech.* **32**, 737–764.

IMBERGER, J. 1980 Selective withdrawal: a review. *IAHR Proc. Second Intl Symp. Stratified Flows, Trondheim, Norway*, vol. 1, pp. 381–400.

IMBERGER, J., THOMPSON, R. O. R. Y. & FANDRY, C. 1976 Selective withdrawal from a finite rectangular tank. *J. Fluid Mech.* **70**, 489–512.

IVEY, G. N. & BLAKE, S. 1985 Axisymmetric withdrawal and inflow in a density-stratified container. *J. Fluid Mech.* **161**, 115–137.

IVEY, G. N. & IMBERGER, J. 1978 Field investigation of selective withdrawal. *J. Hydraul. Div. ASCE* **104**, 1225–1237.

KRANENBURG, C. 1979 Sink flow in a rotating basin. *J. Fluid Mech.* **94**, 65–81.

KRANENBURG, C. 1980 Selective withdrawal from a rotating two-layer fluid. *IAHR Proc. Second Intl Symp. Stratified Flows, Trondheim, Norway*, vol. 1, pp. 401–410.

LAWRENCE, G. A. 1980 Selective withdrawal through a point sink. *IAHR Proc. Second Intl Symp. Stratified Flows, Trondheim, Norway*, vol. 1, pp. 411–423.

MCDONALD, N. R. 1992 Flows caused by mass forcing in a stratified ocean. *Deep Sea Res.* **39**, 1767–1790.

MCDONALD, N. R. & IMBERGER, J. 1991 A line sink in a rotating stratified fluid. *J. Fluid Mech.* **233**, 349–368.

MCDONALD, N. R. & IMBERGER, J. 1992 Withdrawal of a stratified fluid from a rotating channel. *J. Fluid Mech.* **235**, 643–664.

MONISMITH, S. G., IMBERGER, J. & BILLI, G. 1988 Shear-waves and unsteady selective withdrawal. *J. Hydraul. Div. ASCE* **114** (HY9), 1134–1152.

MONISMITH, S. G. & MAXWORTHY, T. 1989 Selective withdrawal and spin-up of a rotating, stratified fluid. *J. Fluid Mech.* **199**, 377–401.

PAO, H. P. & KAO, T. W. 1974 Dynamics of establishment of selective withdrawal of a stratified fluid from a line sink. Part 1. Theory. *J. Fluid Mech.* **65**, 657–688.

PAO, H. P. & SHIH, T. H. 1973 Selective withdrawal and blocking wave in rotating fluids. *J. Fluid Mech.* **57**, 459–480.

PATERSON, A. R. 1983 *A First Course in Fluid Dynamics*. Cambridge University Press.

SPIGEL, R. H. & FARRANT, B. 1984 Selective withdrawal through a point sink and pycnocline formation in a linearly stratified fluid. *J. Hyd. Res.* **22**, 35–51.

WHITEHEAD, J. A. 1980 Selective withdrawal of a rotating stratified fluid. *Dyn. Atmos. Oceans* **5**, 123–135.

WHITEHEAD, J. A. & PORTER, D. L. 1977 Axisymmetric critical withdrawal of a rotating fluid. *Dyn. Atmos. Oceans* **2**, 1–18.

YIH, C. S. 1980 *Stratified Flows*. Academic.